# Electronic Supplementary Information

## Savinase-Functionalised Oxidative Drug-Loaded Nanocarriers Enhance the Treatment of Solid Colorectal Tumours in 3D Cell Culture Model

**Anel Mun,[a,b] Nuriya Nurlankyzy,[a,b] Saule Kalmagambetova,[a] Aidos Baumuratov,[d] Dos Sarbassov,[a,b]**
**Vesselin N. Paunov[e]* and Agata N. Burska[b,c]***

[a] *Department of Life Sciences, School of Sciences and Humanities, Nazarbayev University, Astana, Kazakhstan*

[b] *National Laboratory Astana, Nazarbayev University, Astana, Kazakhstan*

[c] *Department of Biomedical Science, School of Medicine, Nazarbayev University, Astana, Kazakhstan*

[d] *Core Facilities, Nazarbayev University, Astana, Kazakhstan*

[e] *Department of Chemistry, School of Sciences and Humanities, Nazarbayev University, Astana, Kazakhstan.*

** Correspondence: agata.burska@nu.edu.kz, vesselin.paunov@nu.edu.kz*

(***J. Mater. Chem. B. 2025***)

## Contents



| | Contents | Page number |
|---|---|---|
| **I** | Fig. S1A: Absorbance at 880nm of the reaction mixture versus the ATO concentration as a calibration plot for quantification of free ATO in solution. | **S-2** |
| **Ii** | Fig. S1B: Absorbance at 520 nm of the DCPIP/D-VC reaction mixture versus the D-VC concentration as a calibration plot for quantification of free D-VC in solution | **S-3** |
| **Iii** | Fig. S1C: D-VC released versus time | **S-3** |
| **Iv** | Fig. S2: (A) Effect of the ATPS Dex-in-PEO emulsion formation technique on the clusteroids morphology, and (B) Effect of the culture plate coating on the growth of the clusteroids. | **S-4** |
| **V** | Fig. S3: Uniformity of clusteroid size across conditions prior to treatment. | **S-5** |
| **Vi** | Fig. S4: Size distribution of HCT116 clusteroids before and after 48-hour treatment with oxidative drug combinations. | **S-6** |
| **Vii** | Fig. S5: Size distribution of SW620 clusteroids before and after 48-hour treatment with oxidative drug combinations. | **S-7** |
| **Viii** | Fig. S6: Flow cytometry analysis of apoptosis in 3D HCT 116 clusteroids using Annexin V and propidium iodide (PI) staining. | **S-8** |
| **Ix** | Fig. S7: Flow cytometry analysis of apoptosis in 3D SW 620 clusteroids using Annexin V and propidium iodide (PI) staining. | **S-9** |

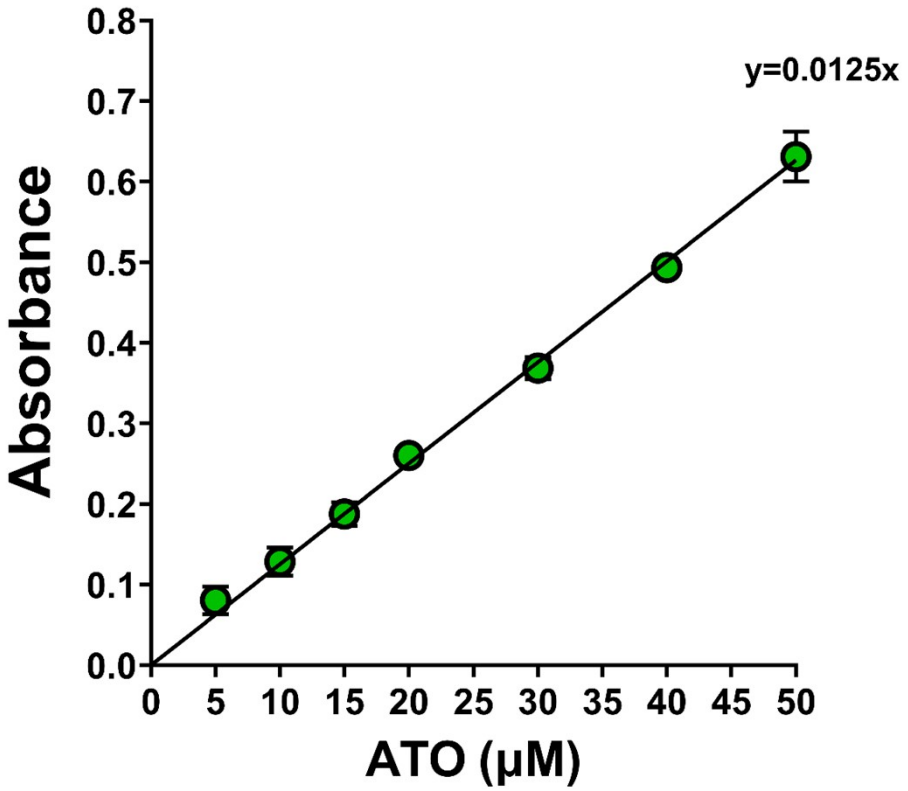


**Fig. S1A:** Absorbance at 880nm of the reaction mixture versus the ATO concentration as a calibration plot for quantification of free ATO in solution using the molybdate method. The calibration and the blank correction are described in the Methods section of the main paper.

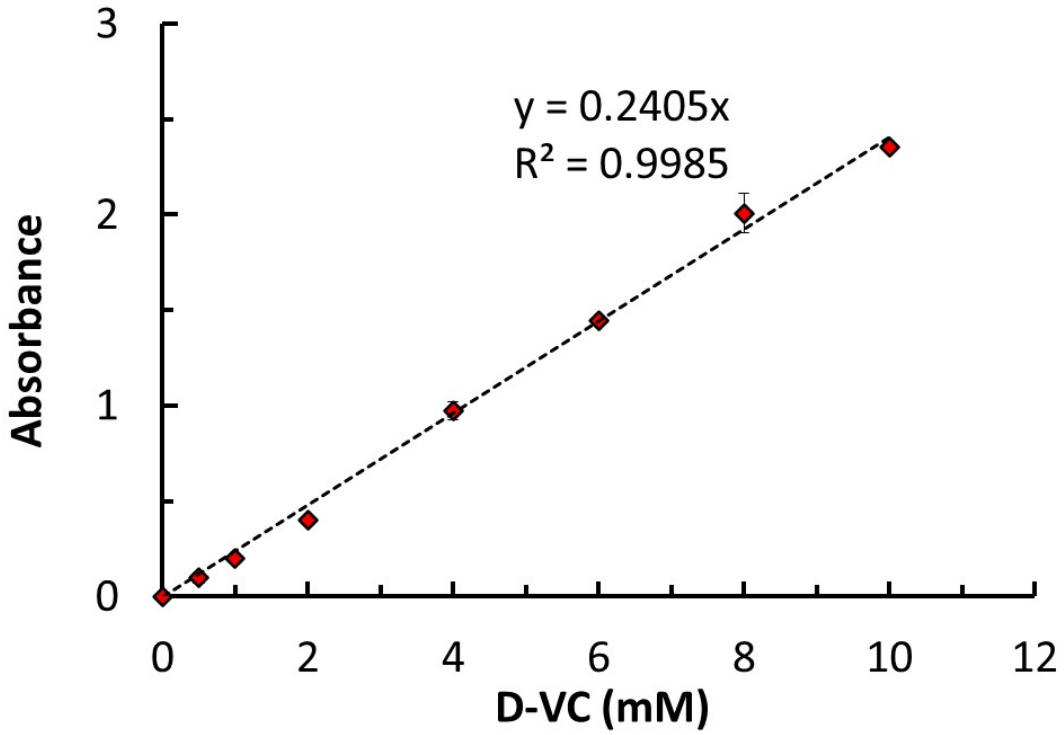


Figure S1B. Absorbance at 520 nm of the DCPIP/D-VC reaction mixture versus the D-VC concentration as a calibration plot for quantification of free D-VC in solution.

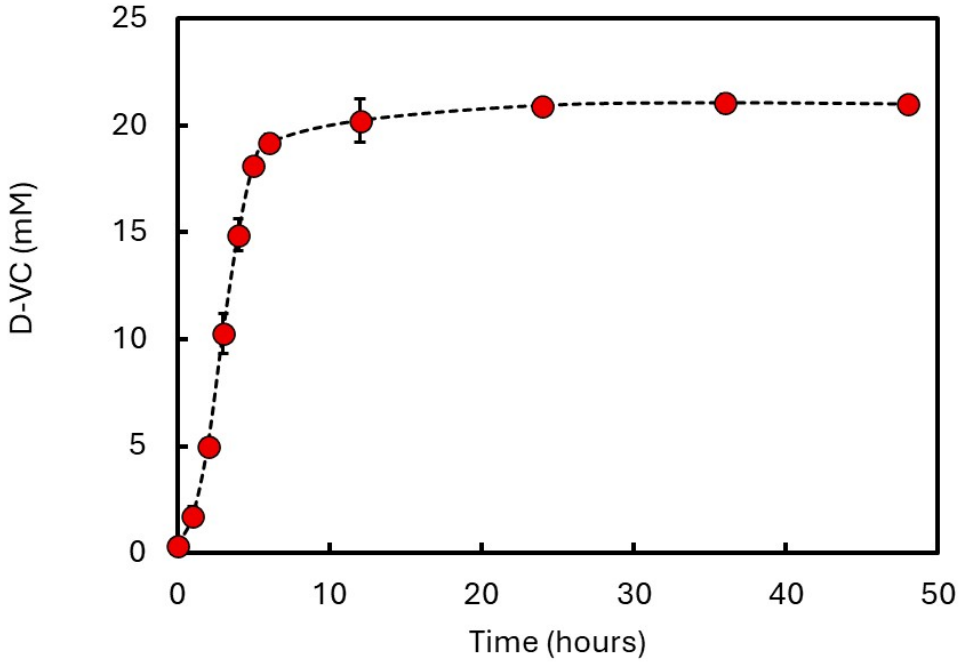


Figure S1C. Kinetics of D-VC release from Sav-NPs in a dialysis setup experiment.

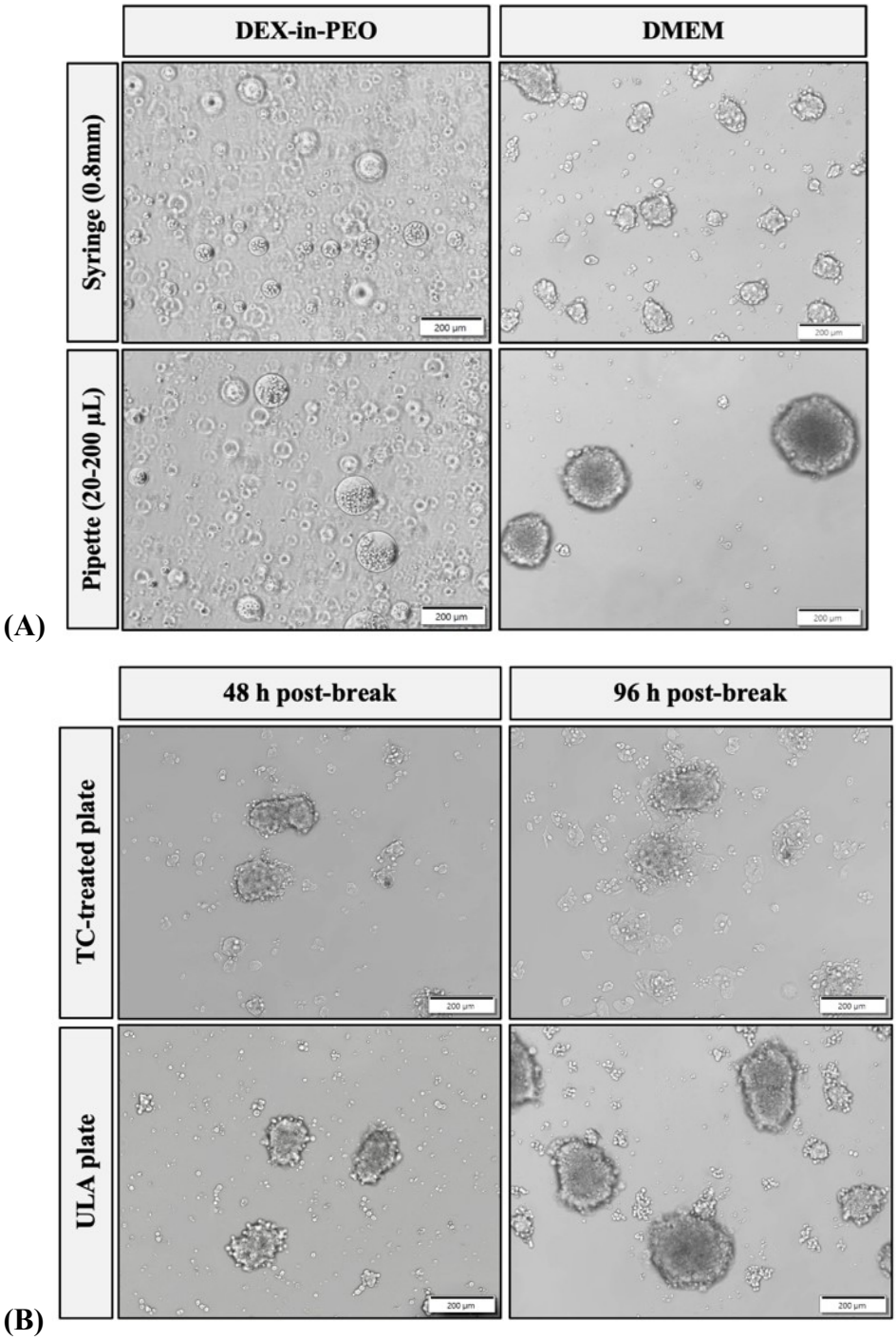


**Fig. S2:** (A) Effect of the ATPS DEX-in-PEO emulsion formation technique on the clusteroids morphology, before and after breaking down of the emulsion with DMEM. The syringe needle-based method produced too-small DEX drops under the experimental conditions to encapsulate the HCT116 cells, while the 1mL pipette homogenization with 2 pumps proved optimal. (B) Effect of the culture plate coating on the growth of the clusteroids. Note that TC-treated plates promote the long-term disintegration of the clusteroids while the ultra-low attachment (ULA) plate preserves the clusteroids' morphology and promotes its growth.

**Clusteroid optimization study**

To establish 3D clusteroid models with optimal size, different emulsification strategies for DEX-in-PEO ATPS emulsion were explored. We adopted a pipette-based emulsification approach, which led to the formation of larger, more compact clusteroids with significantly fewer residual single cells (Fig S2A). These differences became especially evident after emulsion breakage and subsequent 24-hour incubation in DMEM supplemented with 10% FBS (Figure S2A). Next, we evaluated the effect of the well plate surface on the clusteroid maintenance and growth. Clusteroids seeded into standard tissue culture (TC)-treated plates began to adhere, spread and lose their 3D integrity over time (Figure S2B).

In contrast, when seeded into ultra-low attachment (ULA) plates, clusteroids retained their spherical morphology and grew in size while maintaining compactness and structural coherence. Brightfield images captured at 48h and 96 hours post-ATPS emulsion breakage illustrate this contrast in structural preservation (Figure S2B).

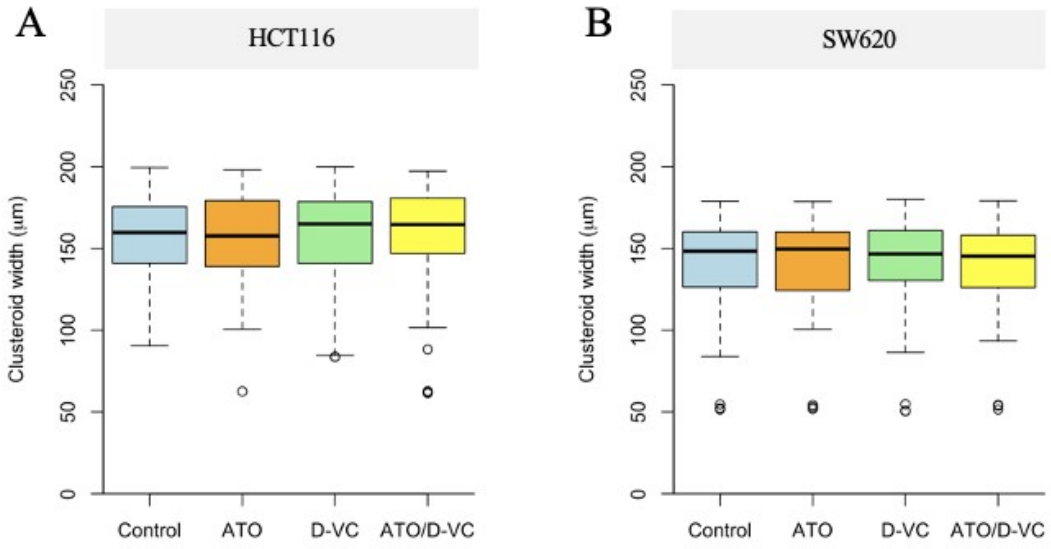


**Fig. S3.** Uniformity of clusteroid size across conditions prior to treatment. (A–B) Box plot analysis of clusteroid size after 48 hours of culture (prior to treatment) for HCT116 (A) and SW620 (B) clusteroids. Conditions include: untreated control, ATO (7.5 µM), D-VC (1.5 mM), and ATO/D-VC combination (7.5 µM / 1.5 mM). Measurements were performed on n=90 clusteroids per condition, collected across three experimental replicates.

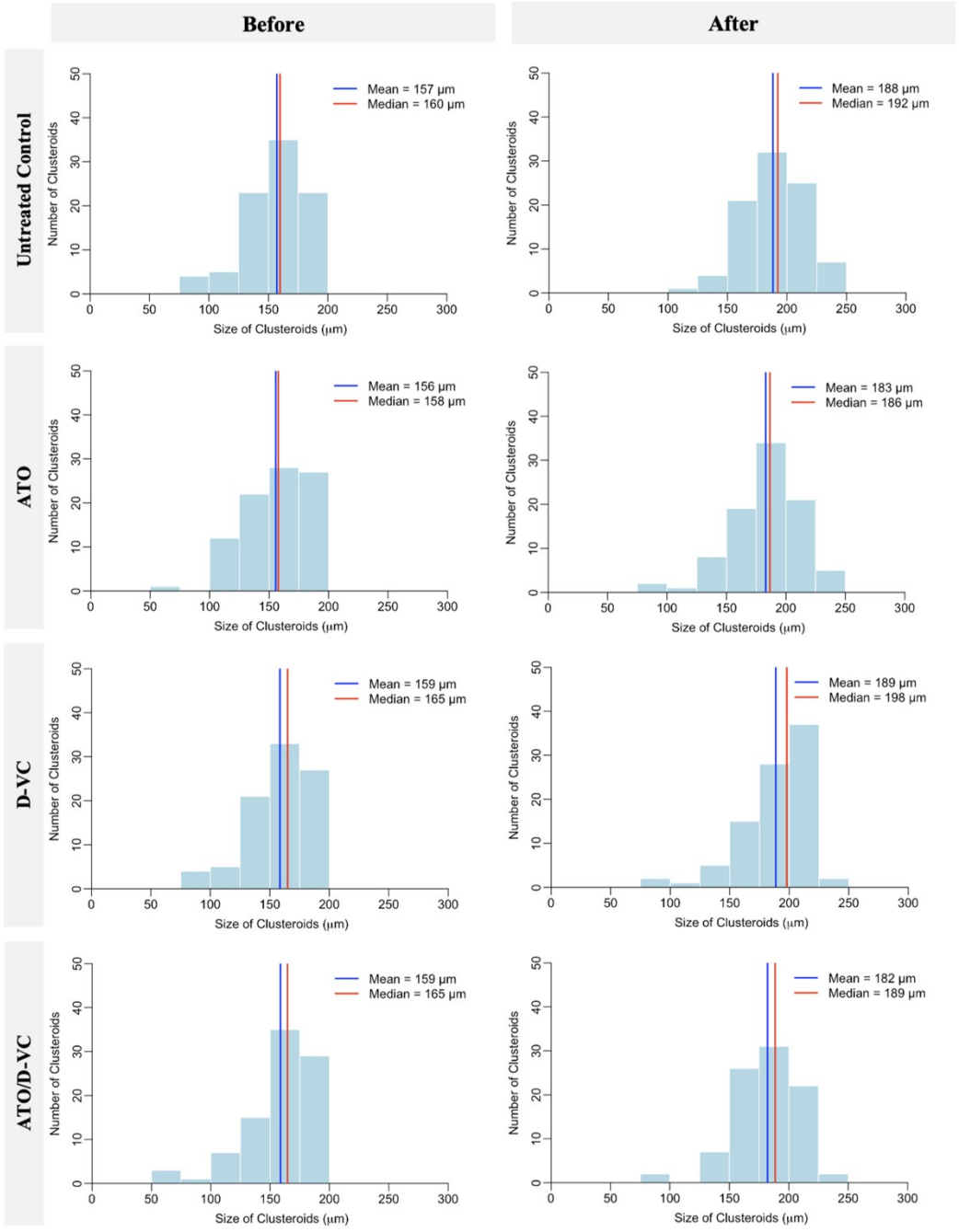


**Figure S4.** Size distribution of HCT116 clusteroids before and after 48-hour treatment with oxidative drug combinations. Histograms show clusteroid diameters across four treatment groups: untreated control, ATO (7.5 µM), D-VC (1.5 mM), and ATO/D-VC combination (7.5 µM / 1.5 mM). "Before" indicates measurements taken prior to treatment, while "After" represents clusteroid sizes following 48 hours of incubation with the respective conditions. Mean (blue line) and median (red line) values are indicated. Measurements were performed on n=90 clusteroids per condition, collected across three independent experimental replicates.

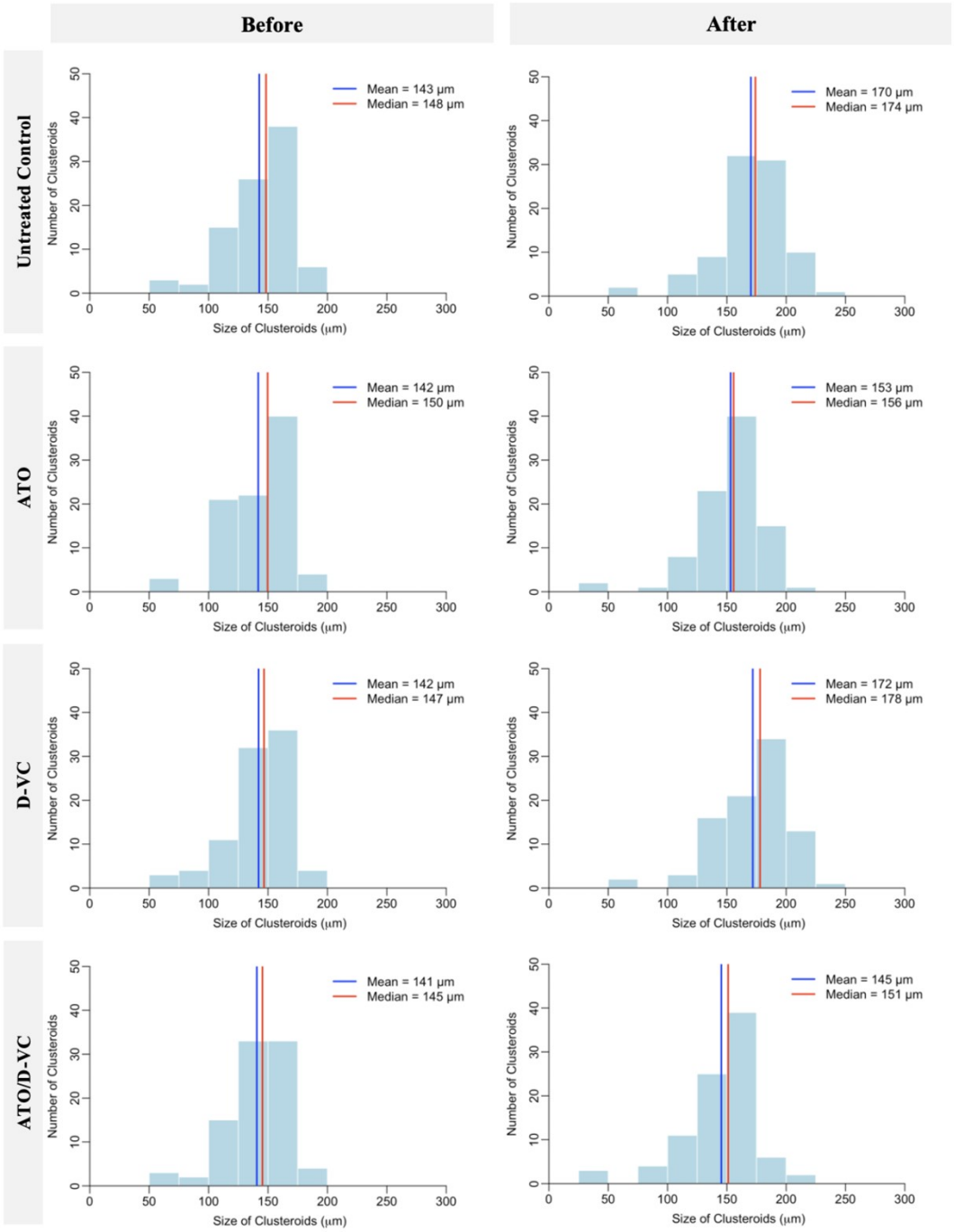


**Figure S5.** Size distribution of SW620 clusteroids before and after 48-hour treatment with oxidative drug combinations. Histograms show clusteroid diameters across four treatment groups: untreated control, ATO (7.5 μM), D-VC (1.5 mM), and ATO/D-VC combination (7.5 μM / 1.5 mM). "Before" indicates measurements taken prior to treatment, while "After" represents clusteroid sizes following 48 hours of incubation with the respective conditions. Mean (blue line) and median (red line) values are indicated. Measurements were performed on n=90 clusteroids per condition, collected across three independent experimental replicates.

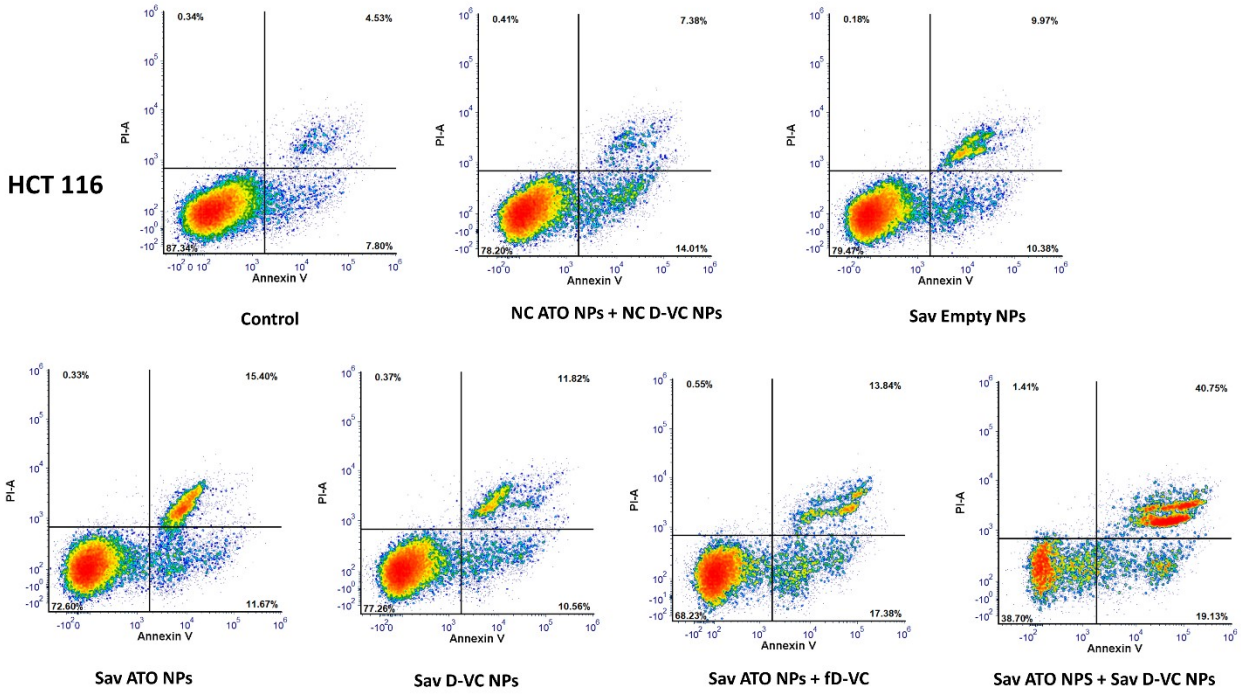


**Figure S6.** Example of flow cytometry analysis of apoptosis in 3D HCT 116 clusteroids using Annexin V and propidium iodide (PI) staining. Representative scatterplots depict the distribution of live (Annexin V−/PI−), early apoptotic (Annexin V+/PI−), late apoptotic/necrotic (Annexin V+/PI+), and dead cells (Annexin V−/PI+) across different treatment groups. Quantification of early (Annexin V+/PI−) and late apoptotic (Annexin V+/PI+) populations reveals a significant increase in apoptosis following treatment with drug-loaded Savinase-coated nanoparticles (NPs), especially in the combination therapy group, where both drugs are in NP form. These results demonstrate the enhanced pro-apoptotic effect of Savinase-coated NP-mediated drug delivery in HCT 116 3D cultures compared to controls.

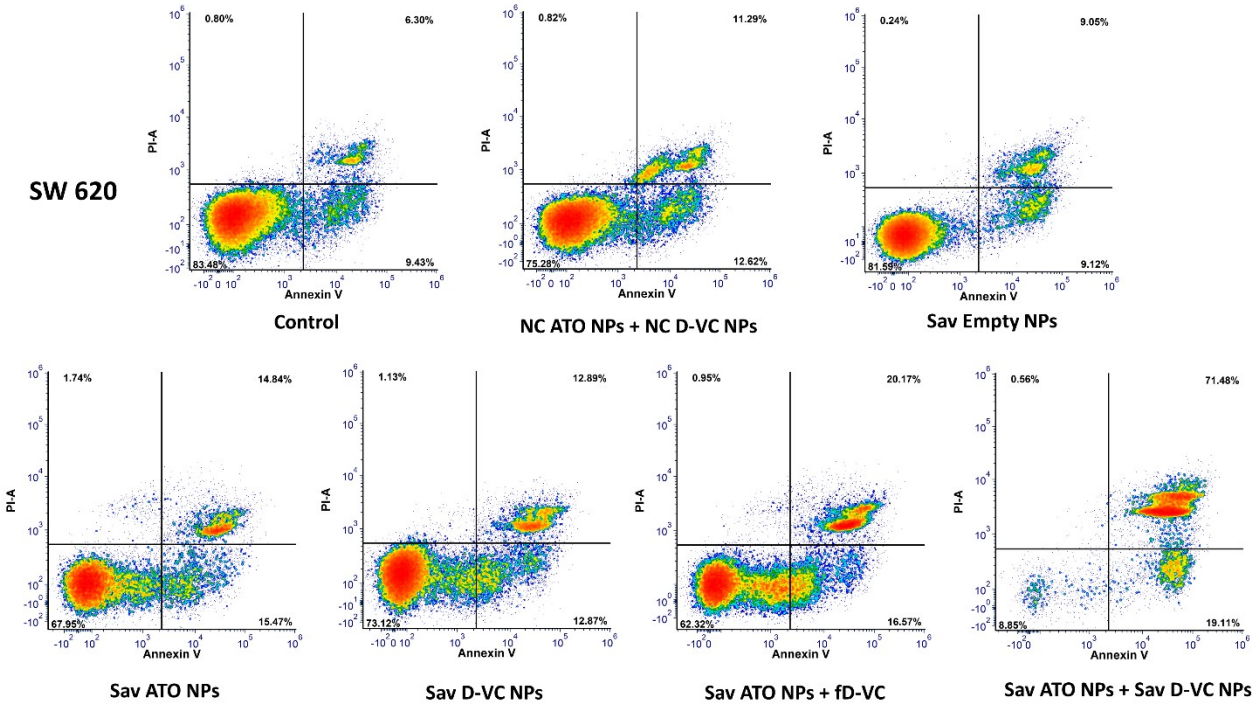


**Fig. S7:** Example of flow cytometry analysis of apoptosis in 3D SW 620 clusteroids using Annexin V and propidium iodide (PI) staining. Representative scatterplots depict the distribution of live (Annexin V−/PI−), early apoptotic (Annexin V+/PI−), late apoptotic/necrotic (Annexin V+/PI+), and dead cells (Annexin V−/PI+) across different treatment groups. Quantification of early (Annexin V+/PI−) and late apoptotic (Annexin V+/PI+) populations reveals a significant increase in apoptosis following treatment with drug-loaded Savinase-coated nanoparticles (NPs), especially in the combination therapy group, where both drugs are in NP form. These results demonstrate the enhanced pro-apoptotic effect of Savinase-coated NP-mediated drug delivery in SW 620 3D cultures compared to controls.